Applications of Small Animal PET

14

Sonja Schelhaas

Contents

14.1 Introduction

Specific accumulation of radioactive tracers can provide insights into physiological processes within a body. Even more meaningful information can be gathered when radioactivity is assessed in a tomographic manner, which also provides information on tumor heterogeneity. These imaged processes comprise functional, metabolic, cellular, and molecular activities. These data can be obtained in a longitudinal manner, enabling evaluation of changes over time. Nuclear medicine approaches to do so comprise single-photon emission computed tomography (SPECT) and positron emission tomography (PET). Both of these methods are already widely used in the field of oncology in the clinical scenario. However, preclinical studies are indispensable for developing new imaging paradigms and understanding the biology underlining specific processes, as preclinical setups harbor potentials of

S. Schelhaas (✉)
European Institute for Molecular Imaging, University of Münster, Waldeyerstr. 15, 48149 Münster, Germany
e-mail: sonja.schelhaas@uni-muenster.de

O. Schober et al. (eds.), *Molecular Imaging in Oncology*,
Recent Results in Cancer Research 216,
https://doi.org/10.1007/978-3-030-42618-7_14

image validation by ex vivo analyses. Those are only exceptional in the clinical situation. Here, we will focus on small animal PET. Aspects covering preclinical SPECT are described in the chapter "Preclinical SPECT and SPECT-CT".

PET relies on exogenous application of a positron-emitting substance. During the radioactive decay, a proton is converted to a neutron, while also a positron (e^+) is released. The positron undergoes an annihilation reaction with a nearby electron (e^-), resulting in the emission of two high-energy photons (γ-rays, 511 keV each) which are emitted in exactly opposing directions. The simultaneous detection (within a few nanoseconds) of this pair of photons by the detector allows the determination of the line of incidence (also called line of response) facilitating the reconstruction of the source of radioactivity. The degree of the two emitted photons is not always exactly 180°, based on the residual momentum of the positron and the electron at the time of annihilation. This non-colinearity (± 0.25°) and also the fact that the positron particles travel a certain distance in tissue before the annihilation reaction (positron range, depending on the radionuclide and its energy spectrum) lead to limitations in the maximal achievable spatial resolution [10, 30].

There is no depth limitation in the detection of γ-rays. The half-life of the isotopes used for PET can differ from minutes (e.g., ^{15}O: 2 min, ^{11}C: 20 min) to hours (^{68}Ga: 68 min, ^{18}F: 110 min) or days (^{124}I: 4.2 d). Importantly, PET provides a very high detection sensitivity down to picomolar concentrations—which is about two to three orders of magnitude higher than for SPECT [39]. Hence, the amount of the radioactive substances applied is very low (tracer principle), and there is almost no interference with normal regular processes underlying the tracer accumulation or the body physiology.

In this chapter, we will give an overview of small animal PET imaging with regard to (i) challenges, and its applications in oncology in the fields of (ii) tumor characterization, (iii) therapy response evaluation, and (iv) therapy development.

14.2 Challenges of Small Animal PET

There are several aspects that have to be considered when applying small animal PET imaging, especially with respect to potential transfer of results to humans. First of all, the size of animal models is smaller than the size of humans. This bears technical challenges, as a spatial resolution of ∼1 cm, which is usually achieved with clinical scanners, is not suitable to image processes within mice or rats. For this need, dedicated small animal PET cameras have been developed, which have a spatial resolution of ∼1 mm [58]. One example of a small animal PET scanner is depicted in Fig. 14.1.

The reduced blood volume of rodent models in comparison to humans also has implication on the volume that can be injected into the animal. These volumes are generally regulated by national institutions, such as the USDA in the US or the GV-SOLAS in Germany. Especially in the context of small animal PET imaging, this is of importance. The half-life of the radiotracers employed for PET is in general

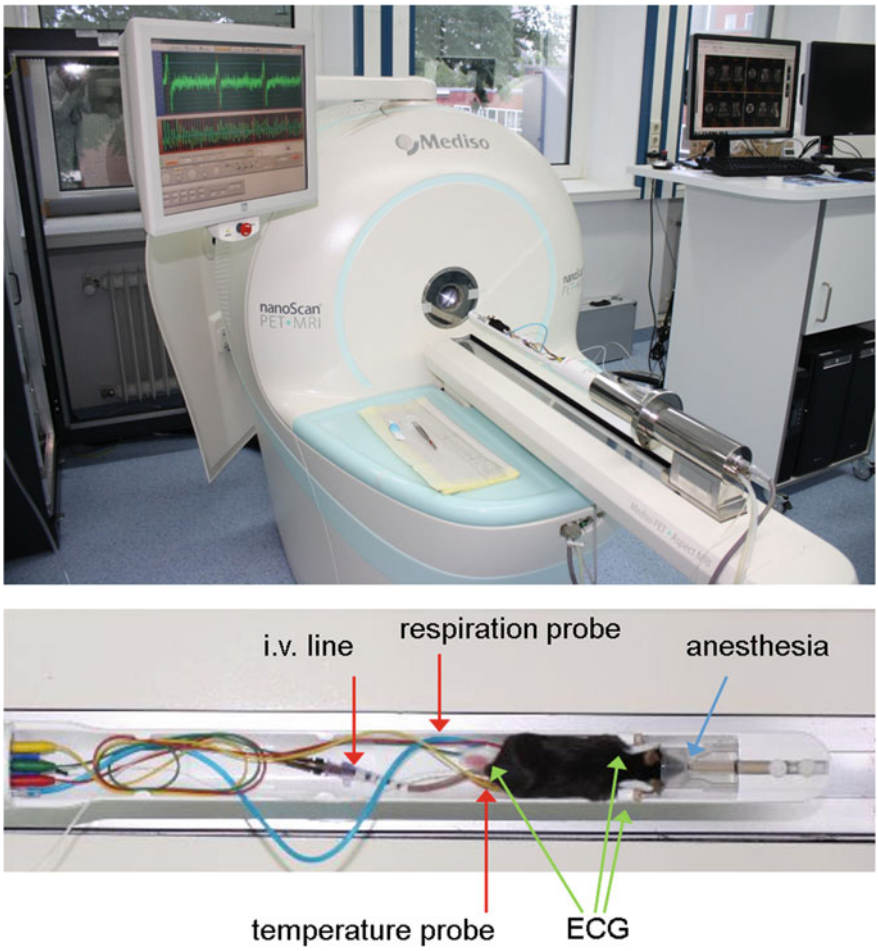

Fig. 14.1 Example of a small animal PET camera and a respective animal cradle. Depicted is a combined PET/MR system. Most modern preclinical PET cameras allow arrangement of the narcotized mouse on an animal bed equipped with respiration, heartbeat (ECG), and temperature control

relatively short. Due to the radioactive decay, the amount of the tracer might have to be increased for animals injected at a later time point. This does not only affect the total volume, which can impact pharmacology or physiology, but also the amounts of solvents like ethanol increase, potentially resulting in undesirable side effects.

Upon that, breathing and heart rate, as well as metabolism differ between humans and rodents. Consequently, the distribution of radioactive tracers might differ between species. The biodistribution of 3'-Deoxy-3'-^{18}F-Fluorothymidine (^{18}F-FLT) may serve as an example. This thymidine analog visualizes cellular

proliferation. Due to differences in thymidine levels in blood as well as in thymidine metabolism, the biodistribution of ^{18}F-FLT also differs. For example, accumulation of ^{18}F-FLT in the liver is low in dogs compared to humans [47] and the biodistribution in mice was reported to vary in different strains [32]. This does not imply that results obtained in animals cannot be transferred to patients. However, species-specific differences might have to be considered.

To obtain sufficient PET image quality, image acquisition has to occur in the range of minutes. While this is no issue in adult patients, which can lie still in a scanner for this period of time, this is a challenge in small animal imaging. There are approaches to perform PET imaging in awake rodents [62]. However, in general, the animals are immobilized by means of narcosis. The narcotic agent can potentially interfere with blood flow, tissue oxygenation, body temperature, and metabolism of an organism and hence with the distribution of a tracer. This has been well studied with ^{18}F-FDG. For instance, warming of anesthetized animals diminishes accumulation of this tracer in brown fat tissue [16], and the choice of narcosis affects insulin levels. This in turn regulates blood glucose concentrations and consequently ^{18}F-FDG uptake [27]. Figure 14.2 shows a mouse undergoing an

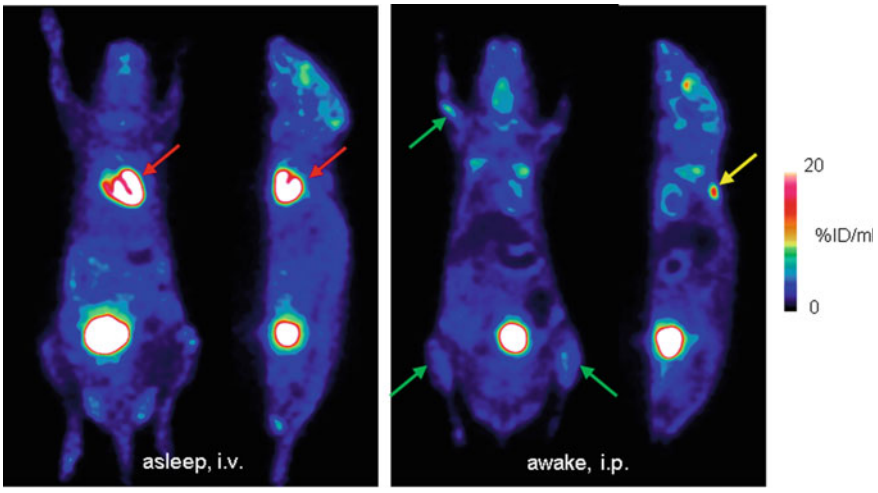

Fig. 14.2 Choice of narcosis affects distribution of ^{18}F-FDG in a C57/BL6 mouse. Images show two ^{18}F-FDG PET studies of the same mouse where each PET acquisition was performed under isoflurane narcosis 50–60 min after injection of 10 MBq ^{18}F-FDG. In the first example (left panel), ^{18}F-FDG injection and biodistribution took place under isoflurane anesthesia, while the mouse was positioned on a heating mat. In the second example (right panel), ^{18}F-FDG was injected intraperitoneally (i.p.) in an awake mouse. Coronal and sagittal planes focusing on the heart are shown here. Note the increased ^{18}F-FDG uptake of the myocardium under isoflurane narcosis (red arrows), resulting from altered glucose metabolism and effects of the narcotic agents on perfusion [11]. Brown fat (yellow arrow) is not visible in the PET images if the mouse was warmed during the tracer uptake period [16]. The increased activity of skeletal muscles of awake mice is reflected by increased ^{18}F-FDG uptake (green arrows)

^{18}F-FDG PET scan under different narcotic conditions. These data show that it is important to carefully consider animal handling conditions and keep them constant during the course of an experiment. Also, hypothermia of the animals must be avoided and fasting can be an important issue when dealing with ^{18}F-FDG.

A further issue that has to be considered when performing preclinical PET is radiation exposure, especially when serial imaging in combination with CT is performed. The whole-body dose of a single PET scan is in the range of 0.06–0.9 Gy for mice and 0.01–0.27 Gy for rats [17]. Radiation doses resulting from CT scans highly depend on the instrument settings and range from 0.017 Gy–0.78 Gy [8]. These values are not negligible, taking into account that the lethal dose for 50% of a population 30 d after whole-body irradiation ($LD_{50/30}$) is in the range of 5 Gy for mice [19]. Exact values vary with mouse strain and age. Gene expression can already be altered with doses as low as 0.2 Gy [2]. Hence, effects of PET/CT imaging on experimental outcome cannot be excluded.

The setup of the infrastructure for small animal PET imaging might be challenging. This method requires positron-emitting isotopes. Hence, especially when using short-lived radiotracers, a nearby cyclotron and the respective radiochemistry have to be localized in close proximity. Furthermore, the equipment is very expensive, and there is a need for the setup of a radioactive control area. Last but not least, the logistics of the animals might be a hurdle, especially when performing longitudinal studies. Many research institutes are depending on a central animal facility. Due to hygiene and in general legislative restrictions, and also due to radiation limits, transport of animals back to this central facility is not always possible. Consequently, adequate animal housing might have to be implemented within the institution.

One additional hurdle in small animal PET imaging is the choice of the animal model. As it is a model, it is in itself artificial and can resemble the situation in a human being only to a limited extend. One also has to keep in mind that therapies that address issues of the host organism, such as vascularization or the immune system, might act differently in rodents and other animals. For oncology research, there exist various mouse tumor models [13, 41]. Most commonly, xenograft models are used. For these, tumor cells, mostly originating from human cancers, are cultivated in vitro and transferred to an immunocompromised mouse, either ectopically (mostly subcutaneously), orthotopically (in the usual position, like gliomas in the brain), or systemically. These tumors are less heterogeneous than patient cancer tissues. However, this also makes animal experiments more reproducible than results obtained from more heterogeneous samples. Moreover, the cell lines can be genetically modified, enabling the evaluation of the importance of specific genes for tumor development or tracer accumulation. The microenvironment of tumor xenografts does not quite resemble the clinical situation, especially in the case of subcutaneous tumor implantation. Patient-derived xenograft (PDx) models, which are directly originating from clinical tumor samples, are supposed to more closely resemble the heterogeneity observed in patients. For most of these models, the use of immunocompromised mice is necessary, as the host immune system would successfully fight the cancer. Allografts (cells derived from

the same species) can be implanted in a similar manner, and the host can be immunocompetent.

In the clinical scenario, the potential of malignant tumors to spread and form metastases is in general associated with a poor prognosis. The differentiation level of metastasized tumor cells often differs from the primary tumor, thereby complicating the choice of an adequate therapy. To mimic and investigate the metastatic behavior of tumors in a preclinical setting is challenging. Injection of tumor cells into the bloodstream does not resemble metastasis-initiating steps. When working with primary tumors, these are in general growing so fast that the animal has to be sacrificed before metastases are detectable. One possible approach is to surgically remove the primary tumor and follow the metastases in the upcoming weeks [6]. There also exists a range of genetic engineered mouse models (GEMMs) of cancer in immunocompetent mice. In many instances, these more closely resemble the nature of human cancers, ranging from tumor initiating steps to metastasis formation [25].

14.3 Tumor Characterization

Assessment of tumor biology is a crucial step in understanding the disease and developing novel therapies. What is the vascularization state? Is there an overexpression of a specific antigen? These questions might arise and be of fundamental importance for the success of a diagnostic or therapeutic approach. Consequently, characterization of a tumor in a non-invasive manner by means of PET can provide information on metabolic modifications of a cancer over time and can aid in deciding for a treatment paradigm. Especially when employing multiple modalities, profiling of a tumor is possible. In general, features of cancers, which could potentially be imaged, are mostly related to the hallmarks of cancers, as summarized by Hanahan and Weinberg [20].

In the clinical setting, PET imaging does have a prominent role in detection, diagnosis, and staging of tumors. For preclinical models, tumor detection and follow up in itself might be of less value than in the clinic, as in most instances the localization is known, and the size itself can be assessed by more easily accessible methods, such as CT. However, tracers used for clinical cancer diagnostics do in one way or another also provide information on characteristics of tumors.

The rate of aerobic glycolysis in tumors is generally high due to the Warburg effect [51, 53]. Hence, tumors make use of glucose from the extracellular space and consequently take up glucose analogs, such as fluorodeoxyglucose (^{18}F-FDG). ^{18}F-FDG is the most commonly used PET tracer for clinical molecular imaging and has applications in detection, staging, and therapy response assessment. Also in the preclinical setting, it has been used for the analysis of tumor engraftment or metastasis detection. Figure 14.3 shows ^{18}F-FDG PET images of a mouse with subcutaneous tumors. PET visualizes the growth of the tumor over time in terms of metabolic tumor volume (MTV), which parallels tumor volumes as assessed by

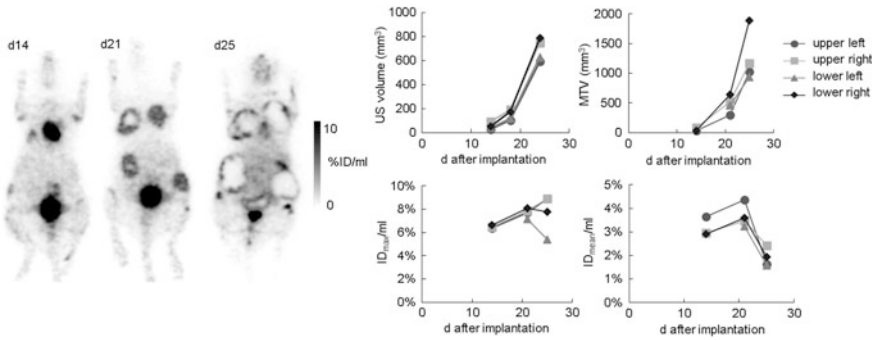

Fig. 14.3 ^{18}F-FDG PET imaging to monitor tumor growth. Coronal planes of ^{18}F-FDG PET images of a nude mouse harboring four subcutaneous U87 glioblastomas are shown here at different days (d) after tumor implantation. Tumor volumes as measured by ultrasound (US) are increasing during the course of time, which is also reflected in the metabolic tumor volume (MTV) assessed on the PET images. The amount of central necrosis visible on the PET images is increasing during tumor growth, resulting in decreasing mean radiotracer uptake

ultrasound (US). In this experimental setup, maximal tracer uptake (expressed as percent injected dose: $\%ID_{max}$/ml) is mostly unaffected by tumor growth, while average tracer uptake in the tumor (here expressed as $\%ID_{mean}$/ml) is decreasing with increasing tumor size. The latter is related to an increase in necrosis within the tumors, which is visible on the PET images. Hence, these data show that the mode of data analysis should be wisely chosen.

Not only (anaerobic) glycolysis, but many metabolism pathways are deregulated in cancers. Consequently, a range of tracers have been developed to visualize processes such as amino acid transport (L-[methyl-^{11}C]methionine (^{11}C-MET) or *O*-(2-[^{18}F]fluoroethyl)-L-tyrosine (^{18}F-FET)), fatty acid synthesis (^{11}C-acetate), membrane phospholipid synthesis (^{11}C-choline), or proliferation (^{18}F-FLT) [31, 54].

The vasculature is of crucial importance for delivery of nutrients and oxygen to tissues. In the case of tumor development, as soon as the tumor reaches a size of a few millimeters, there is a need for the development of new vasculature, which is characterized by increased permeability, increased vessel diameter, and delayed maturation [4]. As angiogenesis might be an attractive target for tumor therapy, there is a need to non-invasively monitor the angiogenic state of a tumor. Key regulators are $\alpha_v\beta_3$ integrins and the vascular endothelial growth factor (VEGF). $\alpha_v\beta_3$ integrins are upregulated during angiogenesis. Small peptides containing an arginine–glycine–aspartic acid (RDG) sequence are ligands of $\alpha_v\beta_3$ and might serve as lead structures for $\alpha_v\beta_3$ targeting tracers, such as ^{18}F-FRGD2 [61]. Also, radiolabeled VEGF has been successfully employed to monitor the vascularization in a preclinical setup [7]. The perfusion itself can be assessed by tracers like $H_2^{15}O$ [3].

Vascularization has an impact on the oxygen level within tumors. Oxygen consumption of tumors is generally high, whereas the oxygen supply might be low, potentially resulting in hypoxic conditions within a tumor. Hypoxia is associated

with tumor aggressiveness, risk of metastasis formation, or treatment resistance [49]. Hence, imaging of hypoxia might be helpful for tumor characterization and therapy decisions. ^{18}F-labeled nitroimidazoles are reduced to reactive intermediary species binding to intracellular proteins in hypoxic cells. ^{18}F-FMISO (^{18}F-fluoromisonidazole) is the most widely used hypoxia imaging agent, which accumulates in tissue when $pO_2 < 10$ mm Hg [36].

Characterization of a tumor by means of PET can be helpful in patient stratification. In a recently published study, Sun et al. designed a radiotracer (*N*-(3-chloro-4-fluorophenyl)-7-(2-(2-(2-(2-^{18}F-fluoroethoxy) ethoxy) ethoxy) ethoxy)-6-methoxyquinazolin-4-amine, ^{18}F-MPG) that targets a specific mutation in the epidermal growth factor receptor (EGFR). Non-small cell lung cancer models with varying mutations in this receptor showed comparable accumulation of ^{18}F-FDG, whereas uptake of ^{18}F-MPG was in line with the specific EGFR mutation and with response to treatment with the tyrosine kinase inhibitor gefitinib in lung cancer. After this successful preclinical validation, the authors demonstrated that this tracer facilitates clinical treatment decisions [48].

14.4 Evaluation of Therapy Response

PET has the potential to monitor therapeutic effects, ideally before morphological changes in tumor volume are visible. This is because PET can directly visualize processes within a cancer that ultimately can result in a rest in tumor growth or even a morphological shrinkage of the tumor. These processes include tumor proliferation, cell death, and energy metabolism. Therapies might target cells outside a cancer such as the vascularization or immune cells that can also be visualized by PET. Hence, looking beyond the tumor might also provide information on therapeutic effects.

The most widely used PET tracer ^{18}F-FDG has successfully been applied in a range of preclinical studies monitoring therapy response [23]. Reduction in glucose metabolism appears to be a good predictor for treatment response, also in the clinical setting. However, uptake of this tracer is not tumor-specific, as it also accumulates in inflammatory lesions. Tumor therapies can cause massive cell death, which in turn initiates an inflammatory response similar to a wound-healing process [40]. These recruited immune cells might result in a transient increase in ^{18}F-FDG uptake, masking a potential reduction of the glycolytic activity of the tumor [5, 18]. Hence, there is a need for more tumor-specific tracers to evaluate treatment response.

Many tumor therapies have an anti-proliferative effect. Hence, visualization of tumor proliferation is an approach that can be applied to a range of treatment strategies. One of the key steps in tumor cell proliferation is the synthesis of novel DNA strands. Consequently, radiolabeled DNA building blocks might be employed for imaging proliferation. As thymidine is exclusive for DNA (and not RNA), it can be employed for imaging of tumor proliferation. While ^{11}C-thymidine has only a

short half-life and is rapidly degraded in vivo, 3'-deoxy-3-^{18}F-fluorothymidine (^{18}F-FLT) shows superior imaging qualities. It has been used in a range of preclinical and clinical studies, demonstrating a reduction in tracer uptake after therapy in line with treatment response and/or changes in immunohistochemical markers of proliferation [44]. However, when therapeutic agents interfere with the thymidine de novo pathway [28, 42] or compete with thymidine for cellular uptake [46], changes in tracer uptake are uncoupled from changes in proliferation. This demonstrates that a detailed understanding of the mechanism of tracer and drug accumulation is indispensable for an understanding of treatment-induced changes in PET images. Especially this detailed understanding can be gained with preclinical analyses, as imaging findings can easily be corroborated by ex vivo analyses. This is not only true for changes within the solid tumor. Proliferation might also be affected in hematopoietic organs (bone marrow and spleen). Many therapies exert a transient myelosuppressive effect. This effect, and subsequent recovery, is visible on ^{18}F-FLT PET scans, not only in the preclinical setting [45], but also in the clinical scenario [29]. Hence, one should also pay attention to regions outside of the tumor, as the whole-body imaging method PET can show a whole lot more than a single lesion.

Tumor therapy often induces apoptosis, a form of cell death, which is accompanied by a range of morphological and biochemical alterations, such as phosphatidylserine (PS) externalization, caspase-3 activation, DNA degradation, and cellular shrinkage. These targets harbor potential for molecular imaging. When imaging caspase activation, the tracer has to be able to cross the cell membrane, due to the intracellular localization of the target. Isatin-5-sulfonamide (^{18}F-ICMT11) is one example of a PET radiotracer targeting activated caspase-3 [34]. Alterations occurring on the cell surface of cells undergoing apoptosis can be detected, e.g., with 2-(5-fluoro-pentyl)-2-methyl-malonic acid (^{18}F-ML-10) [14] or with radiolabeled annexin V [38, 57]. However, reports on treatment monitoring with cell death tracers are limited, implying that this is a field that needs further improvement.

14.5 Therapy Development

What is the anatomical distribution of a specific therapeutic agent? Does it accumulate within a primary tumor or metastases? Next to the therapy-induced impact on the tumor biology, these are questions that can potentially be answered by PET and they are of special interest in preclinical evaluations of novel treatment approaches.

Drug delivery systems, like liposomes or nanoparticles, can be designed in a way to contain a PET radioisotope [9]. Drugs might also be directly labeled with a radionuclide. ^{11}C-labeling of DNA-intercalating agents was helpful in preclinical evaluation of the most promising candidates for future clinical applications [35]. Mathematical modeling of tissue distribution from dynamic PET scans can provide further information on free concentrations or clearance from plasma to tissue [33].

However, blood concentration (plasma input function) of the radiotracer has to be known for accurate quantitative analysis, usually derived from arterial blood sampling, which is challenging in rodents due to their limited blood volume. Image-derived input functions can serve as an alternative.

When analyzing the distribution of a radiolabeled drug, one has to keep in mind that the radiolabel might affect the drug in terms of activity, affinity, or pharmacokinetics. Moreover, the distribution within a body also depends on the concentration of a specific agent. Hence, larger concentrations than tracer amounts are necessary for reliable predictions.

Also, cells might be used for the therapy of cancers. For instance, stem cells can be employed to deliver therapeutic agents [12, 60]. Non-invasive detection and tracking of these applied cells can provide information on the accumulation of the cells and therewith the therapeutic agent. For all cell tracking approaches, it is crucial to verify that the labeling does not interfere with the mode of action of the cells. For instance, proliferation or activation patterns can potentially be altered. These issues have to be evaluated beforehand, which is usually done by in vitro assays. Cell tracking also holds great promise for immunotherapies, which employ the host immune system to detect and fight the cancer. This approach might make use of cells that are infused into the subject (adoptive cell transfer). These cells can be visualized by PET by different means [15, 59]. They can be labeled directly with a radioactive agent, such as ^{64}Cu-pyruvaldehyde-bis(N4-methylthiosemicarbazone) (^{64}Cu-PTSM) [1] or ^{89}Zr-Oxine [43]. These approaches are relatively easy and straightforward. However, they have the drawback that the cells can only be tracked for a limited period of time, due to the limited radioactive half-life of the tracers. But even when employing long-lived radioactive isotopes, the radioactivity can leak out of the cells and will be diluted when cells are dividing.

Specific tracers can also aid in visualizing cells. These tracers might target cell surface-specific molecules, e.g., ^{64}Cu-radiolabeld anti-CD4 and anti-CD8 cys-diabodies targeting T cells [50] or radiolabelled interleukin-2 (IL-2) targeting the corresponding IL-2 receptor (CD25) highly expressed on activated T cells [21].

The use of reporter genes is an alternative approach to visualize externally transfused cells. For this purpose, the cells have to be genetically manipulated to express the respective gene, which triggers the accumulation of radiotracers. This gene might code either for an enzyme (such as herpes simplex virus thymidine kinase (HSV-TK) accumulating 9-(4-^{18}F-fluoro-3-hydroxymethylbutyl)guanine (^{18}F-FHBG)), a transporter (e.g., sodium iodide transporter, NIS, accumulating ^{18}F-tetrafluoroborate (^{18}F-BF_4)), or a receptor (e.g., dopamine D2 receptor, accumulating 3-(2'-^{18}F-fluoroethyl)spiperone (^{18}F-FESP)) [56].

Reporter gene approaches can also be applied in the context of gene therapies. For this purpose, DNA encoding for a therapeutic gene is combined with a DNA encoding for an imaging gene. Hence, cells expressing the gene of interest can be visualized by imaging. By this means, it can be evaluated if the gene therapy vector reaches its target specifically and the gene delivery protocol can be optimized in

terms of route of application, timing, or dosing [52]. In a theranostic approach, Jacobs et al. showed that HSV-TK expression as determined by ^{18}F-FHBG PET correlates with glioma response to ganciclovir therapy, a prodrug activated by HSV-TK [22]. The imaging gene, as well as the therapeutic gene, can also be controlled by regulatory elements, allowing visualization of specific inducible processes [55].

14.6 Multimodal PET Imaging

One of the major drawbacks of PET is the fact that no morphological information is provided by this method, making the localization of signals challenging. For this reason, PET is often performed in combination with computer tomography (CT). Upon that, (pre)clinical PET-MR scanners are on the rise. The morphological information can aid in the definition of regions of interest (ROIs) used for quantification and facilitate the exact measurement of organ sizes. CT and MR can not only provide information on anatomy, but they can also aid in attenuation or motion correction and also report on other molecular processes, such as cell death, as described in detail in the respective chapters. This complementary information not only stands for its own, but a direct overlay of these images provides useful information on tumor biology. By performing simultaneous PET-MRI, the group of Pichler demonstrated that areas of high ^{18}F-FLT overlap with areas of fast contrast agent enrichment in T1-weighted MR images, representing viable tumor regions as identified by immunohistochemistry [24]. Moreover, coregistration of PET and MR images acquired in the same imaging session allows for voxel-wise comparison of the data obtained by these two modalities as demonstrated in Fig. 14.4. PET has recently also been used in combination with ultrafast ultrasound, allowing the simultaneous coregistration of tumor vasculature with metabolism during tumor growth [37].

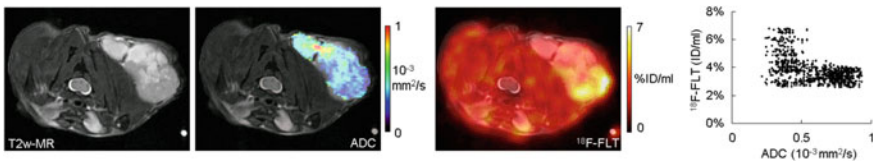

Fig. 14.4 Coregistration of PET and MR images allows identification of relationships between the different modalities on a voxel-wise basis. T2-weighted MR image (left panel) allows detection of a subcutaneous Colo-205 tumor implanted subcutaneously on the right shoulder in a CD1 nude mouse on an anatomical level. The apparent diffusion coefficient (ADC) determined by diffusion-weighted MRI shows variability of water diffusion, as an indicator of cell death. In this tumor, ADC negatively correlates with proliferation determined by ^{18}F-FLT PET (Pearson correlation coefficient = –0.50, $P < 0.0001$)

14.7 Conclusion

As the incidence of oncological diseases is on the rise, due to the increasing age of our population, there is a need for a mechanistic understanding of the processes underlying tumor development and therapies. PET imaging is a valuable tool to non-invasively and longitudinally monitor tumors and treatment-induced changes on a functional level, facilitating personalized cancer therapies. Preclinical experiments are helpful in defining novel imaging or therapy approaches, especially as in vivo results can be corroborated by ex vivo analyses. There is still a need for improved animal models, better reflecting the situation in patients. The future in preclinical PET imaging will most likely be largely influenced by advances in (automated) image analysis, comprising also the analysis of advanced features by means of radiomics [26] and the mathematical modeling in a holistic approach (systems biology).

References

1. Adonai N, Nguyen KN, Walsh J et al (2002) Ex vivo cell labeling with 64Cu-pyruvaldehyde-bis(N4-methylthiosemicarbazone) for imaging cell trafficking in mice with positron-emission tomography. Proc Natl Acad Sci 99:3030–3035
2. Amundson SA, Bittner M, Meltzer P et al (2001) Induction of gene expression as a monitor of exposure to ionizing radiation. Radiat Res 156:657–661
3. Beaney RP, Lammertsma AA, Jones T et al (1984) Positron emission tomography for in-vivo measurement of regional blood flow, oxygen utilisation, and blood volume in patients with breast carcinoma. Lancet (London, England) 1:131–134
4. Bergers G, Benjamin LE (2003) Tumorigenesis and the angiogenic switch. Nat Rev Cancer 3:401–410
5. Brepoels L, Stroobants S, Verhoef G et al (2009) (18)F-FDG and (18)F-FLT uptake early after cyclophosphamide and mTOR inhibition in an experimental lymphoma model. J Nucl Med 50:1102–1109
6. Bulk E, Hascher A, Liersch R et al (2008) Adjuvant therapy with small hairpin RNA interference prevents non-small cell lung cancer metastasis development in mice. Cancer Res 68:1896–1904
7. Cai W, Chen K, Mohamedali KA et al (2006) PET of vascular endothelial growth factor receptor expression. J Nucl Med 47:2048–2056
8. Carlson SK, Classic KL, Bender CE, Russell SJ (2007) Small animal absorbed radiation dose from serial micro-computed tomography imaging. Mol Imaging Biol 9:78–82
9. Chakravarty R, Hong H, Cai W (2014) Positron emission tomography image-guided drug delivery: current status and future perspectives. Mol Pharm 11:3777–3797
10. Cherry SR (2004) In vivo molecular and genomic imaging: new challenges for imaging physics. Phys Med Biol 49:R13–R48
11. Cicone F, Viertl D, Quintela Pousa AM et al (2017) Cardiac radionuclide imaging in rodents: a review of methods, results, and factors at play. Front Med 4:35
12. Corsten MF, Shah K (2008) Therapeutic stem-cells for cancer treatment: hopes and hurdles in tactical warfare. Lancet Oncol 9:376–384
13. de Jong M, Essers J, van Weerden WM (2014) Imaging preclinical tumour models: improving translational power. Nat Rev Cancer 14:481–493

14. Demirci E, Ahmed R, Ocak M et al (2017) Preclinical evaluation of 18F-ML-10 to determine timing of apoptotic response to chemotherapy in solid tumors. Mol Imaging 16:1536012116685941
15. Fruhwirth GO, Kneilling M, de Vries IJM et al (2018) The potential of in vivo imaging for optimization of molecular and cellular anti-cancer immunotherapies. Mol Imaging Biol 20:696–704
16. Fueger BJ, Czernin J, Hildebrandt I et al (2006) Impact of animal handling on the results of 18F-FDG PET studies in mice. J Nucl Med 47:999–1006
17. Funk T, Sun M, Hasegawa BH (2004) Radiation dose estimate in small animal SPECT and PET. Med Phys 31:2680–2686
18. Graf N, Herrmann K, Numberger B et al (2013) [18F]FLT is superior to [18F]FDG for predicting early response to antiproliferative treatment in high-grade lymphoma in a dose-dependent manner. Eur J Nucl Med Mol Imaging 40:34–43
19. Grahn D, Hamilton KF (1957) Genetic variation in the acute lethal response of four inbred mouse strains to whole body X-irradiation. Genetics 42:189–198
20. Hanahan D, Weinberg RA (2011) Hallmarks of cancer: the next generation. Cell 144:646–674
21. Hartimath SV, Draghiciu O, van de Wall S et al (2017) Noninvasive monitoring of cancer therapy induced activated T cells using [18 F]FB-IL-2 PET imaging. Oncoimmunology 6: e1248014
22. Jacobs AH, Rueger MA, Winkeler A et al (2007) Imaging-guided gene therapy of experimental gliomas. Cancer Res 67:1706–1715
23. Jensen MM, Kjaer A (2015) Monitoring of anti-cancer treatment with (18)F-FDG and (18) F-FLT PET: a comprehensive review of pre-clinical studies. Am J Nucl Med Mol Imaging 5:431–456
24. Judenhofer MS, Wehrl HF, Newport DF et al (2008) Simultaneous PET-MRI: a new approach for functional and morphological imaging. Nat Med 14:459–465
25. Kersten K, de Visser KE, van Miltenburg MH, Jonkers J (2017) Genetically engineered mouse models in oncology research and cancer medicine. EMBO Mol Med 9:137–153
26. Lambin P, Rios-Velazquez E, Leijenaar R et al (2012) Radiomics: extracting more information from medical images using advanced feature analysis. Eur J Cancer 48:441–446
27. Lee K-H, Ko B-H, Paik J-Y et al (2005) Effects of anesthetic agents and fasting duration on 18F-FDG biodistribution and insulin levels in tumor-bearing mice. J Nucl Med 46:1531–1536
28. Lee SJ, Kim SY, Chung JH et al (2010) Induction of thymidine kinase 1 after 5-fluorouracil as a mechanism for 3'-deoxy-3'-[18F]fluorothymidine flare. Biochem Pharmacol 80:1528–1536
29. Leimgruber A, Moller A, Everitt SJ et al (2014) Effect of platinum-based chemoradiotherapy on cellular proliferation in bone marrow and spleen, estimated by 18F-FLT PET/CT in patients with locally advanced non-small cell lung cancer. J Nucl Med 55:1075–1080
30. Levin CS, Hoffman EJ (1999) Calculation of positron range and its effect on the fundamental limit of positron emission tomography system spatial resolution. Phys Med Biol 44:781–799
31. Lewis DY, Soloviev D, Brindle KM (2015) Imaging tumor metabolism using positron emission tomography. Cancer J 21:129–136
32. Mankoff DA, Shields AF, Krohn KA (2005) PET imaging of cellular proliferation. Radiol Clin North Am 43:153–167
33. Matthews PM, Rabiner EA, Passchier J, Gunn RN (2012) Positron emission tomography molecular imaging for drug development. Br J Clin Pharmacol 73:175–186
34. Nguyen Q-D, Challapalli A, Smith G et al (2012) Imaging apoptosis with positron emission tomography: 'Bench to bedside' development of the caspase-3/7 specific radiotracer [18F] ICMT-11. Eur J Cancer 48:432–440
35. Osman S, Rowlinson-Busza G, Luthra SK et al (2001) Comparative biodistribution and metabolism of carbon-11-labeled N-[2-(dimethylamino)ethyl]acridine-4-carboxamide and DNA-intercalating analogues. Cancer Res 61:2935–2944
36. Padhani AR, Krohn KA, Lewis JS, Alber M (2007) Imaging oxygenation of human tumours. Eur Radiol 17:861–872

37. Provost J, Garofalakis A, Sourdon J et al (2018) Simultaneous positron emission tomography and ultrafast ultrasound for hybrid molecular, anatomical and functional imaging. Nat Biomed Eng 2:85–94
38. Qin H, Zhang M-R, Xie L et al (2015) PET imaging of apoptosis in tumor-bearing mice and rabbits after paclitaxel treatment with (18)F(-)Labeled recombinant human His10-annexin V. Am J Nucl Med Mol Imaging 5:27–37
39. Rahmim A, Zaidi H (2008) PET versus SPECT: strengths, limitations and challenges. Nucl Med Commun 29:193–207
40. Rock KL, Kono H (2008) The inflammatory response to cell death. Annu Rev Pathol 3:99–126
41. Ruggeri BA, Camp F, Miknyoczki S (2014) Animal models of disease: Pre-clinical animal models of cancer and their applications and utility in drug discovery. Biochem Pharmacol 87:150–161
42. Saito Y, Furukawa T, Arano Y et al (2008) Comparison of semiquantitative fluorescence imaging and PET tracer uptake in mesothelioma models as a monitoring system for growth and therapeutic effects. Nucl Med Biol 35:851–860
43. Sato N, Wu H, Asiedu KO et al (2015) ^{89} Zr-Oxine Complex PET cell imaging in monitoring cell-based therapies. Radiology 275:490–500
44. Schelhaas S, Heinzmann K, Bollineni VR, et al (2017) Preclinical applications of 3'-deoxy-3'-[^{18}F]fluorothymidine in oncology - A systematic review. Theranostics 7(1):40–50
45. Schelhaas S, Held A, Bäumer N et al (2016a) Preclinical evidence that 3′-deoxy-3′-[^{18}F] fluorothymidine PET can visualize recovery of hematopoiesis after gemcitabine chemotherapy. Cancer Res 76(24):7089–7095
46. Schelhaas S, Held A, Wachsmuth L et al (2016b) Gemcitabine mechanism of action confounds early assessment of treatment response by 3′-Deoxy-3′-[^{18}F]fluorothymidine in preclinical models of lung cancer. Cancer Res 76(24):7096–7105
47. Shields AF, Grierson JR, Dohmen BM et al (1998) Imaging proliferation in vivo with [F-18] FLT and positron emission tomography. Nat Med 4:1334–1336
48. Sun X, Xiao Z, Chen G et al (2018) A PET imaging approach for determining EGFR mutation status for improved lung cancer patient management. Sci Transl Med 10:eaan8840
49. Tatum JL, Kelloff GJ, Gillies RJ et al (2006) Hypoxia: importance in tumor biology, noninvasive measurement by imaging, and value of its measurement in the management of cancer therapy. Int J Radiat Biol 82:699–757
50. Tavaré R, McCracken MN, Zettlitz KA et al (2015) Immuno-PET of murine T cell reconstitution postadoptive stem cell transplantation using anti-CD4 and Anti-CD8 Cys-diabodies. J Nucl Med 56:1258–1264
51. Vander Heiden MG, Cantley LC, Thompson CB (2009) Understanding the Warburg effect: the metabolic requirements of cell proliferation. Science 324:1029–1033
52. Waerzeggers Y, Monfared P, Viel T et al (2009) Methods to monitor gene therapy with molecular imaging. Methods 48:146–160
53. Warburg O, Wind F, Negelein E (1927) The metabolism of tumors in the body. J Gen Physiol 8:519–530
54. Wester H-J (2007) Nuclear imaging probes: from bench to bedside. Clin Cancer Res 13:3470–3481
55. Winkeler A, Sena-Esteves M, Paulis LEM et al (2007) Switching on the lights for gene therapy. PLoS ONE 2:e528
56. Yaghoubi SS, Campbell DO, Radu CG, Czernin J (2012) Positron emission tomography reporter genes and reporter probes: gene and cell therapy applications. Theranostics 2:374–391
57. Yagle KJ, Eary JF, Tait JF et al (2005) Evaluation of 18F-annexin V as a PET imaging agent in an animal model of apoptosis. J Nucl Med 46:658–666
58. Yao R, Lecomte R, Crawford ES (2012) Small-animal PET: what is it, and why do we need it? J Nucl Med Technol 40:157–165

59. Zeelen C, Paus C, Draper D et al (2018) In-vivo imaging of tumor-infiltrating immune cells: implications for cancer immunotherapy. Q J Nucl Med Mol Imaging 62:56–77
60. Zhang C-L, Huang T, Wu B-L et al (2017) Stem cells in cancer therapy: opportunities and challenges. Oncotarget 8:75756–75766
61. Zhang X, Xiong Z, Wu Y et al (2006) Quantitative PET imaging of tumor integrin alphavbeta3 expression with 18F-FRGD2. J Nucl Med 47:113–121
62. Zhou VW, Kyme AZ, Meikle SR, Fulton R (2008) An event-driven motion correction method for neurological PET studies of awake laboratory animals. Mol Imaging Biol 10:315–324